

Novel metal-free organic dyes containing linear planar 11,12-dihydroindolo [2,3-*a*]carbazole donor for dye-sensitized solar cells: Effects of π spacer and alkyl chain



Hai Zhang^{a,*}, Zhen-E Chen^a, Jiefang Hu^b, Yanping Hong^{c,**}

^a School of Chemistry and Chemical Engineering, Academician Workstation, Zunyi Normal College, Guizhou Zunyi, 563006, China

^b Jiangxi Vocational Technical College of Industry Trade, Nanchang, 330038, China

^c Jiangxi Key Laboratory of Natural Product and Functional Food, College of Food Science and Engineering, Jiangxi Agricultural University, Nanchang, 330045, China

ARTICLE INFO

Keywords:

Dye-sensitized solar cells
Electron donor
Metal-free sensitizer
Co-adsorption

ABSTRACT

Three novel D- π -A type dyes **DC1**–**3**, which consisting of indolo[2,3-*a*]carbazole as donor scaffold linked to the acceptor/anchoring unit cyanoacetic acid via different π -spacers, were successfully designed and synthesized. The structure, photophysical and electrochemical properties, and photovoltaic properties of the three sensitizers were investigated in detail. The results indicate that the donor 11,12-bis(2-ethylhexyl)-11,12-dihydroindolo[2,3-*a*]carbazole with two branched alkyl chains is effective in inhibiting the intermolecular π - π aggregation effects, and the auxiliary alkyl chains in the π -bridge cause the **DC3**-based DSSCs to exhibit higher open circuit voltages than that of the devices based on dye **DC2**. Among all of the devices fabricated with the dyes, the **DC3**-based cells without chenodeoxycholic acid (CDCA) exhibit the best photovoltaic performance, with a short-circuit current density of 10.98 mA cm⁻², an open circuit voltage of 752 mV and a fill factor of 0.725, corresponding to a highest power conversion efficiency of 5.98% in liquid electrolyte.

1. Introduction

A series of environmental pollution problems caused by burning fossil fuels as well as the growing global energy demand make it urgent to develop new and clean energy sources to meet the needs of industrial production and the environment protection. Dye-sensitized solar cells (DSSCs), as a new generation of photovoltaic technology and an alternative and effective solution to the problems mentioned above, have been received remarkable attention in the past 20 years. Up to date, DSSCs based on ruthenium complexes [1–3], porphyrins [4–7] and metal-free organic dyes [8–21] have made great progress and achieved more than 10% power conversion efficiency (PCE), especially metal-free organic dyes have extensively studied due to their variable structure and simple synthesis.

In general, a typical organic sensitizer contains a D- π -A or D-A- π -A framework, of which the π -bridge is the focus of attention, and various new structures have been used as π spacers to gain higher photovoltaic performance. In contrast, the research of electron donor is still far from sufficient. Currently, only a few structures such as triphenylamine [22–30], carbazole [31–34], anthracene [35,36] and

phenothiazine [37–41] have been used as electron donors. Among these donor groups, triphenylamine donor has been widely used by researchers to synthesize numerous high-efficiency sensitizers in view of the structural deformation and the good electron donating ability. However, when reducing molecular aggregation, the non-planar structure of triphenylamine also inevitably decreases the degree of conjugation inside the molecule as well as the electron transporting ability, which is disadvantageous for the dyes to produce a wider absorption band and a higher photocurrent. Therefore, the development of a donor unit with high-efficiency electron transport capability and good ability to inhibit molecular aggregation is an important challenge for researchers.

Based on the above considerations in mind, we prefer to use a fully planarized structure as the donor unit. Besides, considering that the rod-like conjugated structure may be easier to suppress aggregation than the cyclic conjugated structure, herein, the linear planar structure of the indolo[2,3-*a*]carbazole was finally selected as electron donor, and three sensitizers (**DC1**–**3**) were synthesized to evaluate their photovoltaic properties (Fig. 1). To reduce the π - π stacking of the dye molecules, two 2-ethylhexyl groups were integrated to the nitrogen

* Corresponding author.

** Corresponding author.

E-mail addresses: haizhang@vip.sina.com (H. Zhang), xyqjx@163.com (Y. Hong).

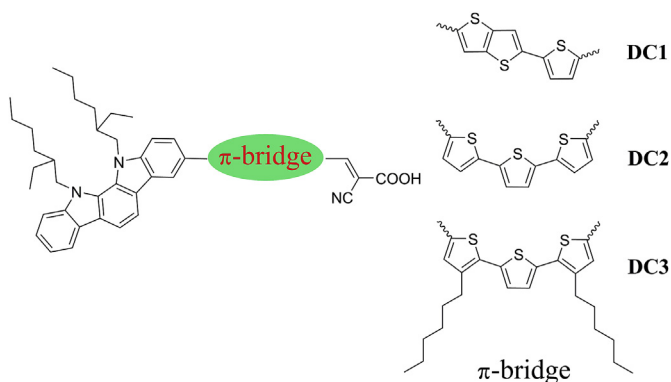


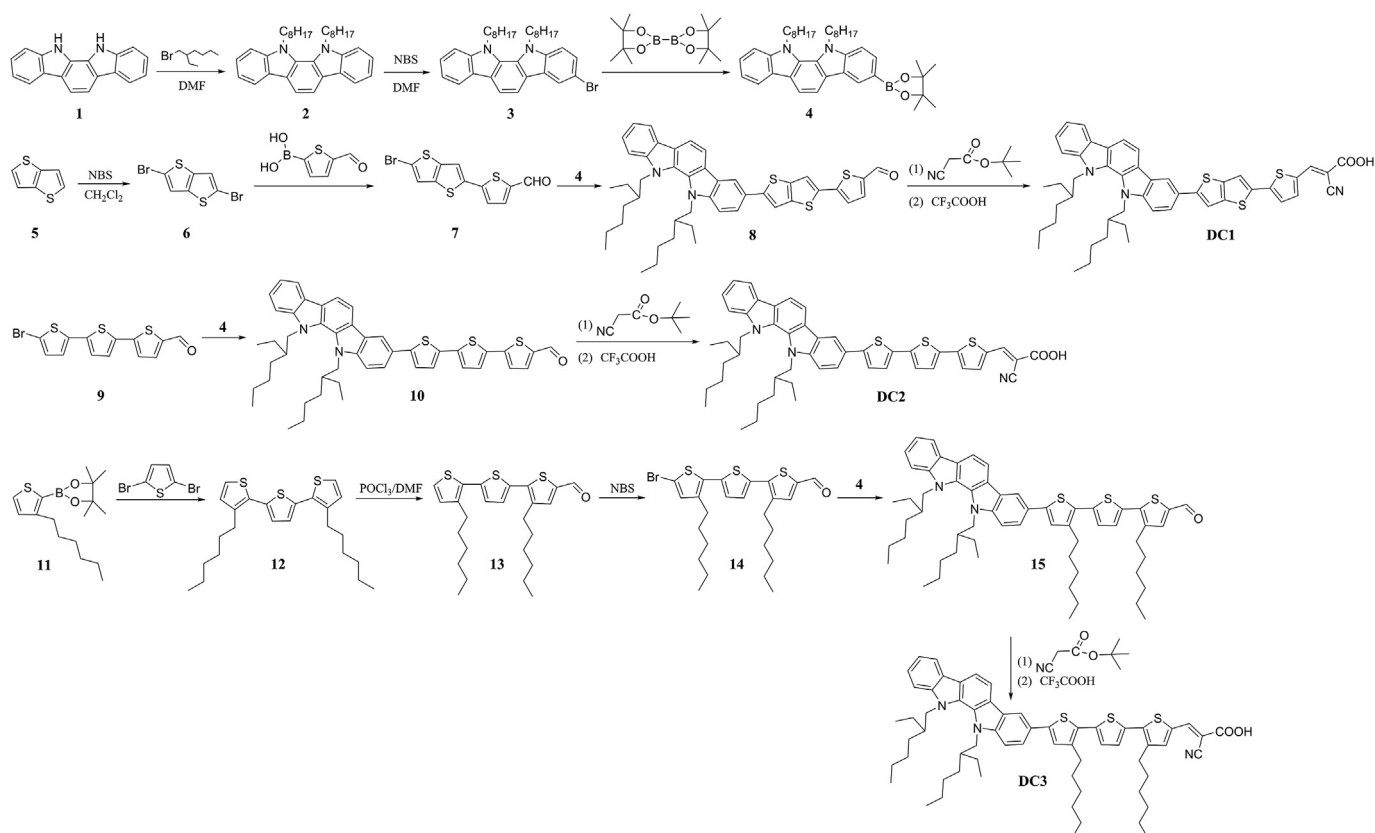
Fig. 1. Chemical structure of the dyes DC1 ~ 3.

atoms in the skeleton of indolo[2,3-*a*]carbazole. In addition, the bridging units of thieno[3,2-*b*]thiophene + thiophene and terthiophene were used to explore the effect of the conjugate mode on the photovoltaic performances of the dyes DC1 and DC2, respectively. At the same time, in order to more effectively inhibit the aggregation of dyes, two auxiliary hexyl groups were further attached to the thiophene ring to obtain the dye DC3.

In this work, in order to understand the influence of this novel planar donor structure on the photoelectric properties of DSSCs, the photophysical, electrochemical and optoelectronic properties of these sensitizers in liquid electrolyte and quasi-solid electrolyte were systematically investigated. Meanwhile, the effect of alkyl chains on inhibition of molecular aggregation was also verified by CDCA co-absorption experiments.

2. Results and discussion

The synthetic routes for DC1 ~ 3 are depicted in Scheme 1. The synthesis of donor unit first involved the alkylation reaction on the dihydroindolocarbazole nitrogen atom and the 2-ethylhexyl chain was introduced into the dihydroindolocarbazole moiety to produce intermediate compound 2 [42]. The bromination of the compound 2 was performed by *N*-bromosuccinimide (NBS) to provide monobrominated compound 3. Then the key intermediate compound, pinacol boronic ester 4, was afforded by coupling of bis(pinacolato)diboron with compound 3. Required precursors 5-(5-bromothiopheno[3,2-*b*]thiophen-2-yl)thiophene-2-carbaldehyde (7) [43] and 5'-bromo-[2,2':5',2''-terthiophene]-5-carbaldehyde (9) [44] were synthesized and purified according to the references. Suzuki-Miyaura cross-coupling reaction of 2-(3-hexylthiophen-2-yl)-4,4,5,5-tetramethyl-1,3,2-dioxaborolane (11) with 2,5-dibromothiophene under modified conditions with tetrakis (triphenylphosphine)-palladium (0) as the catalyst precursor in a biphasic mixture of aqueous K_2CO_3 and THF afforded the compound 12. Subsequent compound 13 was obtained via Vilsmeier-Haak formylation reaction of compound 12, then compound 14 was obtained by bromination reaction of compound 13 using *N*-bromosuccinimide followed by the Michaelis-Arbusov reaction according to the reported literature procedure [45]. In the next step, the corresponding aldehyde intermediates 8, 10 and 15 were obtained by one-step Suzuki coupling reaction. Finally, in the presence of glacial acetic acid and ammonium acetate, these aldehyde derivatives were subjected to Knoevenagel condensation reaction with *tert*-butyl cyanoacetate, respectively, and the products were further hydrolyzed in trifluoroacetic acid to obtain the target dyes. All the new compounds were well characterized by 1H NMR, ^{13}C NMR and HRMS spectra. Peak splitting occurs in some ^{13}C NMR spectra and these values are not counted.



Scheme 1.

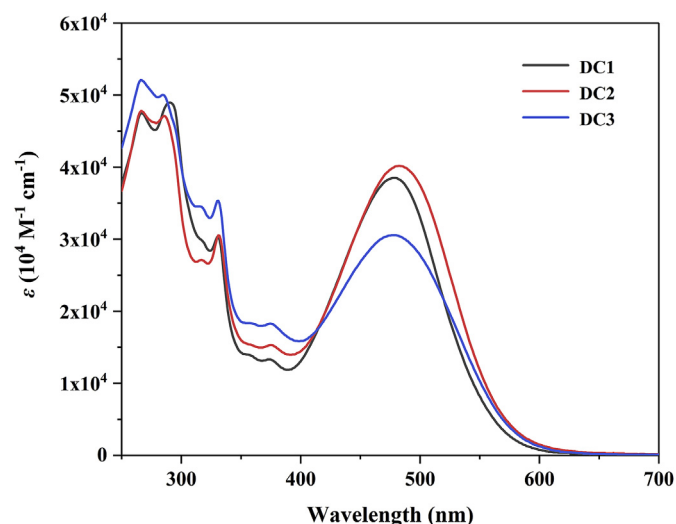


Fig. 2. UV-Vis spectra of DC1–3 in CHCl₃ solution.

2.1. Optical properties

The UV-Vis absorption of the dyes DC1–3 in CHCl₃ solutions are depicted in Fig. 2, and the corresponding data are summarized in Table 1. It can be seen that the absorption spectra of the three dyes are very similar, exhibiting two main absorption bands at 250–350 nm and 400–600 nm, respectively. The former corresponds to the $\pi-\pi^*$ transition of the conjugated system, while the latter can be attributed to the effective charge separation state resulting from intramolecular charge transfer (ICT) between the donor and acceptor moiety. The dye DC2, with terthiophene as the π -bridge, has a red-shift absorption peak ($\lambda_{\max} = 483$ nm) and a higher molar extinction coefficient ($\epsilon = 40100$ M⁻¹ cm⁻¹) compared to those of DC1 ($\lambda_{\max} = 479$ nm, $\epsilon = 38400$ M⁻¹ cm⁻¹). In addition, DC2 is also observed to have a broader range of absorption in the visible region. Compared to those of DC2, however, the absorption spectrum of DC3 is blue-shifted by 4 nm at the maximum absorption wavelength, and it showing a lower molar extinction coefficient. The phenomenon can be attributed to the spatial effect caused by the *n*-hexyl chains attached to the thiophene units.

The fluorescence emission spectra of the three dyes in CHCl₃ are shown in Fig. S20 (in ESI[†]). A blue-shift is observed in the emission spectra of the dye DC2, and the fluorescence intensity of DC1 and DC3 is significantly lowered with respect to DC2. Comparing the π -bridge unit, it can be found that the dye DC1 with thieno[3,2-*b*]thiophene has the strongest fluorescence emission, while when the π -bridge part are the same (DC2 and DC3), the dye DC3 containing two alkyl chains has a distinct red shift. Evidently, DC1 and DC3 show a larger Stokes shift than DC2, which indicates a larger structural difference between the

Table 1

Absorption and Emission Data for organic dyes in CHCl₃.

dye	λ_{\max}^a /nm	ϵ^a /M ⁻¹ cm ⁻¹	λ_{em}^b /nm	λ_{int}^c /nm	E_{ox}^d /V (vs. NHE)	E_{0-0}^e /eV	E_{ox}^{*f} /V (vs. NHE)	E_{HOMO}^g /eV	E_{LUMO}^g /eV
DC1	479	38400	666	569	1.01	2.18	-1.17	-5.11	-2.71
DC2	483	40100	650	551	0.87	2.25	-1.38	-5.04	-2.73
DC3	479	30500	668	575	0.85	2.16	-1.31	-4.94	-2.60

^a Absorption maximum of the dyes measured in CHCl₃ with a concentration of 2×10^{-5} M. ϵ : Molar extinction coefficient at λ_{\max} .

^b Emission maxima of dye in CHCl₃ excited at their $\lambda_{\text{abs}}^{\max}$.

^c λ_{int} ($\lambda_{\text{intersection}}$) obtained from the cross point of normalized absorption and emission spectra in CHCl₃ solution.

^d The ground state oxidation potential (E_{ox}) of dyes were measured in CH₃CN with 0.1 M TBAPF₆ as supporting electrolyte, Fc⁺/Fc as an internal standard, scan rate 50 mV/s.

^e E_{0-0} was estimated from the wavelength at the intersection (λ_{int}) of normalized absorption and emission spectra with the equation $E_{0-0} = 1240/\lambda_{\text{int}}$.

^f The E_{ox}^* was calculated from the equation of $E_{\text{ox}}^* = E_{\text{ox}} - E_{0-0}$.

^g E_{HOMO} and E_{LUMO} by DFT calculation (B3LYP, 6–31 G (d) level).

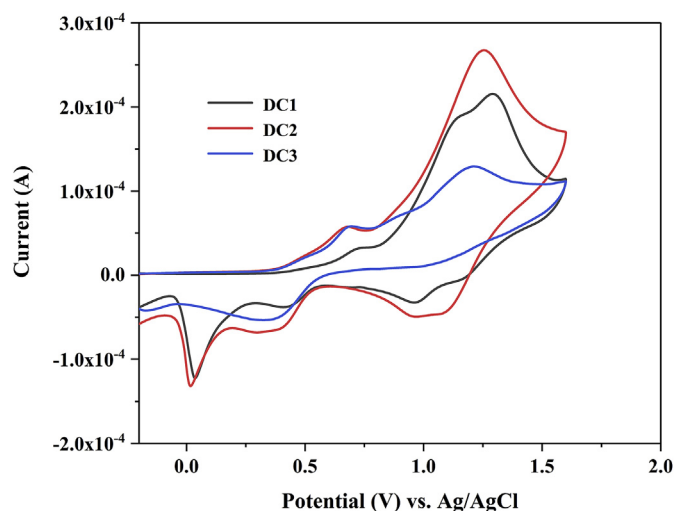


Fig. 3. Cyclic voltammograms curves of DC1–3 and ferrocene/ferrocenium internal reference.

ground and excited states of the molecule (ie, the possibility of forming the charge transfer state), which facilitates hole injection from the D- π -A type dye to the TiO₂ valence band.

2.2. Electrochemical properties

Cyclic voltammogram measurements of dye sensitized films were performed in CH₃CN solution containing 0.1 M TBAPF₆ as the supporting electrolyte with addition of ferrocene as the internal standard. The first oxidation potential vs. NHE (E_{ox}) corresponding to the highest occupied molecular orbital (HOMO vs. NHE) is 1.01, 0.87 and 0.85 V for DC1–3, respectively (Fig. 3, Table 1). Apparently, their E_{ox} are all sufficiently positive than the iodide/triiodide redox couple (0.4 V vs. NHE), indicating that the oxidized dyes generated by the electron injection process can efficiently accept electrons from electrolyte and regenerated. The excitation transition energies (E_{0-0}) (2.18, 2.25 and 2.16 eV for DC1, DC2 and DC3, respectively) are calculated from the intersection points (λ_{int}) of normalized UV-Vis absorption and emission spectra of the sensitizers with the equation $E_{0-0} = 1240/\lambda_{\text{int}}$. The excited-state oxidation potentials (E_{ox}^*) corresponding to the LUMO levels, calculated from $E_{\text{ox}} - E_{0-0}$, are -1.17, -1.38 and -1.31 V for DC1–3 respectively, which are more negative than the conduction band edge of TiO₂ (-0.5 V vs. NHE), indicating that the electron injection process from the photo-excited dye molecule to the conduction band of TiO₂ is energetically permitted.

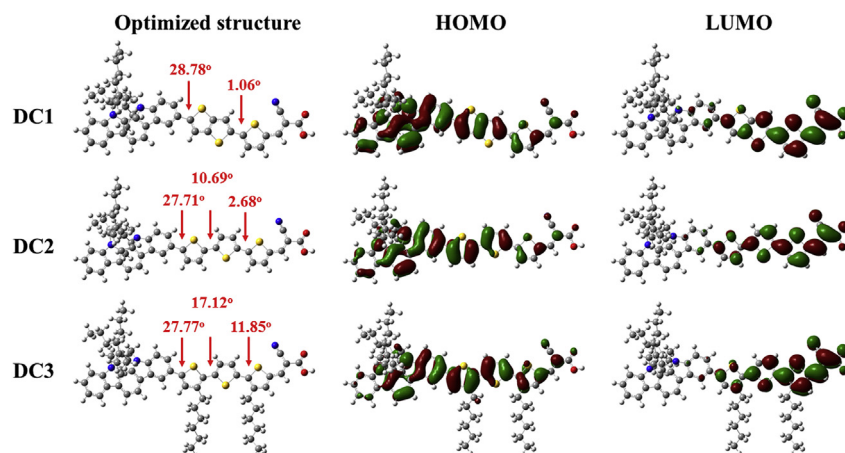


Fig. 4. Optimized structures and electron distributions in HOMO and LUMO levels of DC1–3.

2.3. Theoretical calculations

Density functional theory (DFT) calculations were performed using the Gaussian 09 program suite at the B3LYP/6–31 G(d) level to gain insight into the spatial structure and the frontier orbitals. As shown in Fig. 4, the dihedral angle between the benzene ring and the thieno[3,2-*b*]thiophene ring in sensitizer DC1 is calculated to be 28.78°, while the dihedral angle between the thieno[3,2-*b*]thiophene unit and the neighboring thiophene ring is calculated to be 1.06°. For the sensitizer DC2, when the bridging unit is replaced by terthiophene, the dihedral angle between the benzene ring and the adjacent thiophene ring is 27.71°, and the dihedral angles between the thiophene rings are 10.69° and 2.68°, respectively. Further, when an auxiliary alkyl chain is introduced on two thiophene rings in the sensitizer DC3, these dihedral angles are increased to 27.71°, 17.12° and 11.85°, respectively. It is apparent that the sensitizer DC3 has a more twisted molecular structure than that of DC2 and thus resulting in a worse charge delocalization, which weakens the ICT interaction and is consistent with the absorption spectrum in Fig. 2.

Fig. 4 shows the calculated frontier molecular orbitals of the dyes DC1–3. It can be clearly found that the three dyes have similar characteristics in the spatial distribution of these frontier molecular orbitals, the HOMO levels mainly delocalize on the indolo[2,3-*a*]carbazole moiety with extension to the bridged thiophene moieties, while the LUMO levels are largely π^* with dominating contributions from the π -bridge moiety (thiophene ring) and the acceptor part unit (cyanoacrylic acid). Undoubtedly, the overlap of the HOMO level and the LUMO level facilitates the transfer of charge from the electron donor unit to the electron acceptor unit.

2.4. Photovoltaic properties of DSSCs

The incident photo-current conversion efficiency (IPCE) action spectra and the photocurrent-voltage ($J-V$) curves of liquid electrolyte-based DSSCs on DC1–3 with or without CDCA are collected in Fig. 5. Notably, the device based on dye DC1 shows the highest response at 400–600 nm and a maximum IPCE value of 61% at 450 nm, while the dyes DC2 and DC3 get lower IPCE values of 58% at 420 nm and 58% at 460 nm, respectively, and the dye DC3 exhibits a wider and higher response in the long wavelengths 440–700 nm compared to DC2-based device. The result indicates that the introduction of thieno[3,2-*b*]thiophene or *n*-hexylthiophene instead of the thiophene group in the π -conjugated spacer has a positive effect on IPCE value. The IPCE values of DSSCs co-adsorbed with 0.5 mM CDCA show a similar trend for the three dyes, but are much lower than those of their counterparts, indicating lower short circuit photocurrent densities (J_{sc}).

As seen in Fig. 5b and Table 2, in pure solvent CHCl_3 system without

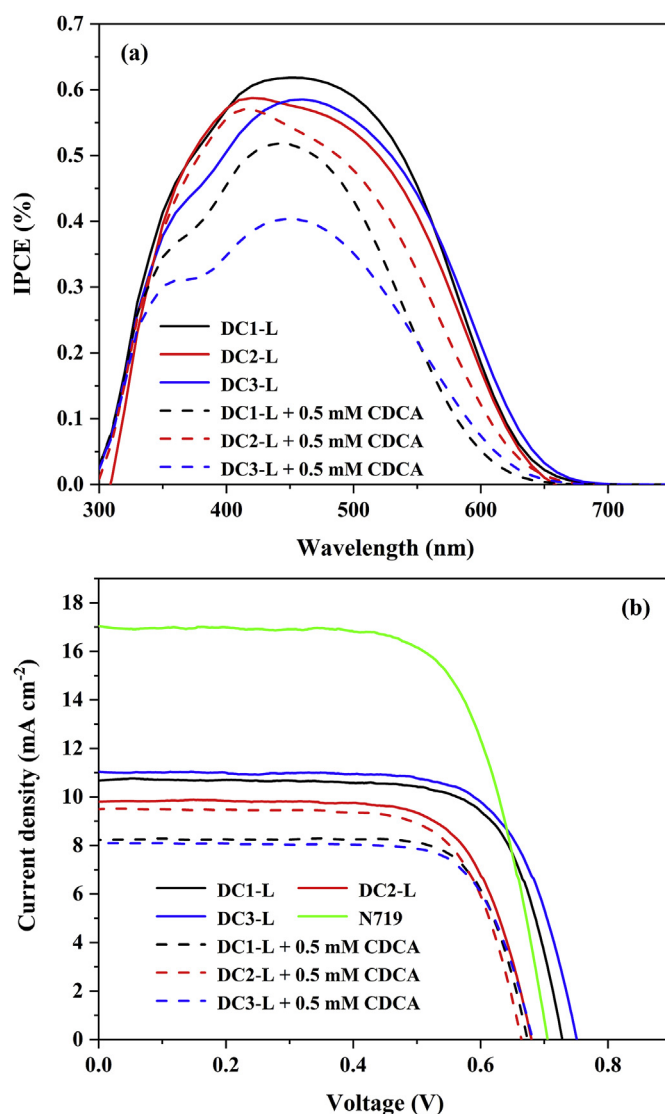


Fig. 5. (a) IPCE action spectra and (b) $J-V$ characteristics of DSSCs based on DC1–3 with liquid electrolyte (L: liquid DSSCs).

CDCA, the DC3-based device gives the best power conversion efficiency (PCE) of 5.98%, having a short circuit photocurrent density (J_{sc}) of 10.98 mA cm^{-2} , an open circuit voltage (V_{oc}) of 752 mV, and a fill

Table 2
Photovoltaic parameters for DSSCs of organic dyes.

Dyes	$V_{oc}^a(V_{oc}^b)/mV$	$J_{sc}^a(J_{sc}^b)/mA\cdot cm^{-2}$	$FF^a(FF^b)/\%$	$PCE^a(PCE^b)/\%$	Dye loading ($mol\ cm^{-2}$)
DC1	729 (731 ± 5)	10.83 (10.73 ± 0.13)	73.21 (73.72 ± 1.32)	5.78 (5.78 ± 0.01)	2.20×10^{-7}
DC2	680 (680 ± 2)	9.73 (9.81 ± 0.08)	79.90 (78.40 ± 1.50)	5.28 (5.23 ± 0.05)	2.35×10^{-7}
DC3	752 (754 ± 3)	10.98 (10.95 ± 0.11)	72.47 (72.31 ± 0.61)	5.98 (5.97 ± 0.01)	1.62×10^{-7}
DC1 + 0.5 mM CDCA	675 (674 ± 1)	8.28 (8.30 ± 0.10)	90.39 (89.22 ± 1.17)	5.05 (4.99 ± 0.10)	1.71×10^{-7}
DC2 + 0.5 mM CDCA	665 (665 ± 1)	9.41 (9.42 ± 0.03)	80.47 (79.94 ± 0.53)	5.04 (5.01 ± 0.03)	2.15×10^{-7}
DC3 + 0.5 mM CDCA	684 (684 ± 2)	8.07 (8.12 ± 0.16)	91.15 (90.15 ± 2.17)	5.03 (5.00 ± 0.03)	6.65×10^{-8}
N719	707 (709 ± 7)	17.28 (17.01 ± 0.32)	68.64 (69.15 ± 0.68)	8.38 (8.34 ± 0.04)	/

TiO₂ thickness 8 + 4 μm and 0.16 cm², [dye] = 0.2 mM, dipping solvent CHCl₃, dipping time 16 h, under AM 1.5 illumination (100 mW/cm²).

^a The best device parameters.

^b The average device parameters (obtained from five devices).

factor (*FF*) of 0.72. Without alkyl chain on the thiophene ring, the device fabricated by DC2 shows a higher *FF* than that of the DSSC based on DC3, whereas the *J*_{sc} and *V*_{oc} of the DC2-cell decrease to 9.73 mA cm⁻² and 680 mV, respectively, resulting in a PCE of 5.28%. With the addition of the CDCA in the dye solution, the performance of the DC1 ~ 3-based devices reduce significantly, exhibiting poorer *J*_{sc} and *V*_{oc} values of (8.28 mA cm⁻², 675 mV), (9.41 mA cm⁻², 665 mV) and (8.07 mA cm⁻², 684 mV), respectively, which lead to inferior PCEs of 5.05%, 5.04% and 5.03%. The results may be attributed to the co-adsorbed CDCA molecules occupying the binding sites on the TiO₂ film, inducing a decrease in the amount of organic dyes loaded on the TiO₂ films. It is clear that the DC3-based device without CDCA obtain both the highest photocurrent and photovoltage, indicating that the alkyl substituted thiophene ring can suppress effectively dye aggregation.

The characteristic *J*–*V* and IPCE curves of DC1 ~ 3 sensitized devices based on quasi-solid-state electrolyte are shown in Fig. 6 and the photovoltaic parameters are listed in Table 3. Compared to liquid electrolyte, the trend of the three curves is the same. QSS-DSSC based on DC1 gives a relatively high IPCE action spectrum with a maximum IPCE value of 66% at 450 nm, and the response range of QSS-DSSCs based on the three dyes are slightly broader compared to the liquid electrolyte. As listed in Table 3, the QSS-DSSC using DC1 as sensitizer gives a PCE of 5.14% with a *J*_{sc} value of 11.08 mA cm⁻², a *V*_{oc} of 682 mV and a *FF* of 0.681. Under the same conditions, the QSS-DSSCs based on DC2 and DC3 obtain *J*_{sc} values of 10.78 and 11.38 mA cm⁻², *V*_{oc} of 655 and 705 mV and *FF* of 0.678 and 0.704, corresponding to PCE values of 4.78 and 5.65%, respectively. Similarly, DC3 shows higher PCE than that of DC1 or DC2 in QSS-DSSCs, which may be attributed to its higher *J*_{sc}, and the fact that the π-bridge groups substituted by *n*-hexyl causes better inhibition of aggregation.

2.5. Electrochemical impedance spectroscopy analysis

Electrochemical impedance spectroscopy (EIS) was next employed in the dark to investigate the electron recombination processes in DSSCs based on the series of DC dyes. EIS analysis of the liquid electrolyte-based DSSCs were performed over the frequency range of 0.1 Hz–10⁶ Hz with an applied bias set at –0.65 V. The small semicircle in the Nyquist plot (Fig. 7) represents the electron transfer from the Pt counter electrode to I₃⁻ ions in the electrolyte, that is, the charge transfer resistance at the Pt/electrolyte interface. The large semicircle in the Nyquist plot indicates the charge recombination between the injected electrons in TiO₂ and I₃⁻ ions in the electrolyte, that is, the charge transfer resistance at the TiO₂/dye/electrolyte interface. The radius of the large semicircle in the middle-frequency region corresponds to the value of the recombination resistance (*R*_{rec}), with a smaller *R*_{rec} value means a larger charge recombination rate. The charge recombination resistance decreases in the order of DC3 > DC1 > DC2, which is in good accordance with the *V*_{oc} values in the DSSCs based on these dyes.

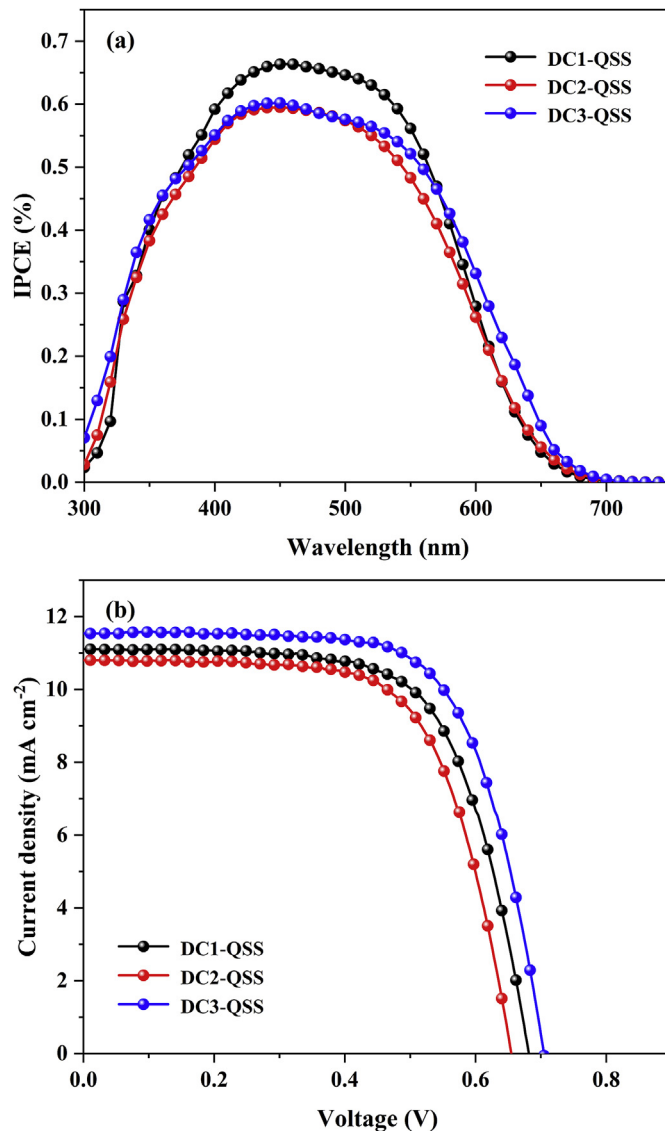


Fig. 6. (a) IPCE action spectra and (b) *J*–*V* characteristics of DSSCs based on DC1 ~ 3 with quasi-solid-state electrolyte (QSS: quasi-solid-state DSSCs).

3. Conclusions

Three novel metal-free sensitizers DC1 ~ 3 have been developed and applied in dye-sensitized solar cells by using a planar indolo[2,3-*a*] carbazole electron donor. In an earlier study, Yi-Zhou Zhu et al. synthesized three sensitizers based on triazatruxene [46]. Due to the larger conjugate plane and the shorter alkyl chain, the photovoltage of devices

Table 3
Photovoltaic parameters for DSSCs of organic dyes.

Dyes	electrolyte	$V_{oc}^a(V_{oc}^b)/mV$	$J_{sc}^a(J_{sc}^b)/mA\cdot cm^{-2}$	$FF^a(FF^b)/\%$	$PCE^a(PCE^b)/\%$
DC1	quasi-solid	682 (684 ± 2)	11.08 (11.07 ± 0.01)	68.05 (67.43 ± 0.62)	5.14 (5.10 ± 0.04)
DC2	quasi-solid	655 (655 ± 1)	10.78 (10.84 ± 0.07)	67.79 (66.93 ± 0.86)	4.78 (4.75 ± 0.05)
DC3	quasi-solid	705 (706 ± 3)	11.38 (11.48 ± 0.10)	70.38 (69.29 ± 1.09)	5.65 (5.62 ± 0.04)

TiO₂ thickness 8 + 4 μm and 0.16 cm², [dye] = 0.2 mM, dipping solvent CHCl₃, dipping time 16 h, under AM 1.5 illumination (100 mW/cm²).

^a The best device parameters.

^b The average device parameters (obtained from five devices).

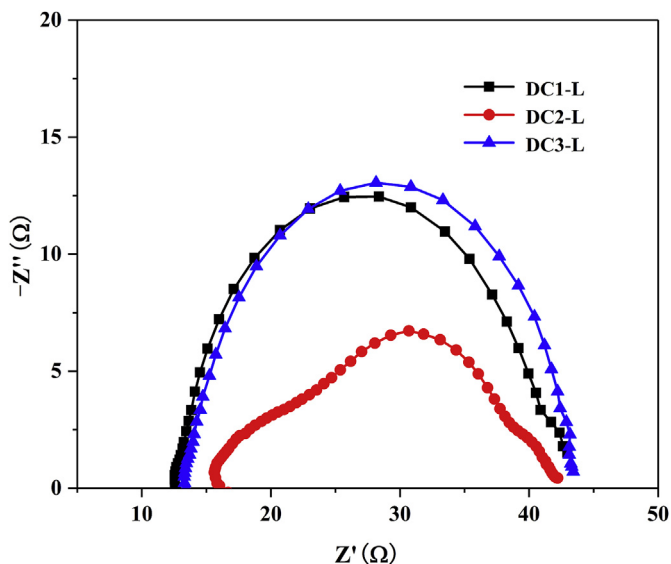


Fig. 7. EIS Nyquist plots for liquid DSSCs based on the three sensitizers measured in the dark under -0.65 V bias (L: liquid DSSCs).

based on the three sensitizers appeared between 654 mV and 686 mV. In addition, several novel indolo[3,2-b]carbazole-based dyes have been reported by He Tian and Linxi Hou et al., respectively [47,48]. In order to inhibit the aggregation of dye molecules, they all chose to introduce two large benzene rings into indolo[3,2-b]carbazole. This strategy has undoubtedly played a good role, devices based on these dyes exhibited higher photovoltages, with the highest photovoltages of 768 mV (DDC1) and 757 mV (QX04). In this study, we tried to inhibit molecular aggregation with a branched alkyl chain of appropriate length. The results show that the molecular aggregation has been effectively suppressed in the dyes **DC1** and **DC2**, which is beneficial to heighten open circuit voltages of the DSSCs based on the two dyes, and the auxiliary alkyl chain as the π -bridge side chain in **DC3** helps to further promote this effect. Therefore, we believe that the introduction of benzene rings or 2-ethylhexyl groups in a rod-shaped donor unit has similar effects on inhibiting molecular aggregation, but the latter synthetic route is obviously simpler.

In conclusion, we have demonstrated for the first time that electron-rich rod structures are promising donor moieties for the development of highly efficient sensitizers, this work provides an alternative direction for rational molecular strategy to achieve high power conversion efficiency, especially to increase electron transfer efficiency and J_{sc} as well as avoiding reducing V_{oc} . Considering the structural characteristics and energy level distribution, it is expected that the D–A– π –A type structure will further improve the light-harvesting ability, and thereby increasing the photocurrent. The relative investigation is undergoing.

4. Experimental

4.1. Measurement and characterizations

¹H and ¹³C NMR spectra of the all intermediate and final products were measured on a Bruker Avance 600 MHz spectrometer by using CDCl₃ or THF-*d*₈ and tetramethylsilane as an internal standard. The mass spectra of the prepared compounds were carried out at Finnigan MAT 95 XP analyzer spectrometer (Thermo Electron Corporation). For melting point XT4B microscopic melting point apparatus was used and uncorrected. UV3600 Plus spectrophotometer (Shimadzu Corporation) and Hitachi F-4600 spectrophotometers were used for the measurement of absorption and fluorescence spectra. Electrochemical redox potentials were measured by Cyclic Voltammetry (CV), using three electrode cells in a one compartment at a scan rate of 50 mV/s. The Ag/AgCl in KCl (3 M) solution and an auxiliary platinum wire were utilized as reference and counter electrode, respectively, while dye coated TiO₂ films were used as working electrode. Tetra-*n*-Butylammonium Hexafluorophosphate ($n\text{-C}_4\text{H}_9$)₄NPF₆ 0.1 M in CH₃CN was used as supporting electrolyte. The photocurrent-voltage (J – V) characteristics of the DSSCs were measured by Keithley 2400 source meter under simulated AM 1.5 G (100 mW/cm²) illumination with a solar light simulator (Pecell-L15, Japan) without mask. A 1 KW Xenon arc lamp (Oriel) served as a light source and its incident light intensity was calibrated with a BS-520 standard silicon solar cell. The incident monochromatic photon-to-current conversion efficiency (IPCE) spectra of the DSSCs were conducted by illuminating monochromatic light from 300 to 800 nm on the basis of a PEC-S20 action spectrum measurement system. The electrochemical impedance spectroscopy (EIS) was conducted on the CS16X electrochemical workstation (Wuhan, China) in dark condition for analyzing the internal impedance characteristics of DSSCs by fitting the impedance spectra using Z-view software. Dye load amount on the films was measured by desorbing with 0.1 M NaOH in THF/H₂O (1:1) and measured by UV–Vis spectrum.

4.2. Fabrication of DSSCs

The working electrode composed of mesoporous TiO₂ layer (8 μm nanocrystalline transparent layer and 4 μm scattering layer) on FTO glass was prepared according to previous reported procedure [49]. The active area of the TiO₂ film was controlled to be 0.4 × 0.4 cm² for photovoltaic performance measurements. The TiO₂ films were immersed into a solution of the dyes (0.2 mM dye in CHCl₃) for 16 h, namely sensitization. The liquid electrolyte used in this work was composed of 0.6 M 1-methyl-3-propylimidazolium iodide (PMII), 0.1 M guanidinium thiocyanate, 0.07 M I₂, 0.05 M LiI, and 0.5 M *tert*-butylpyridine. Sodium lauryl sulfate, ammonium persulfate, sodium hydrogencarbonate and deionized water were heated and stirred in a constant temperature water bath, and nitrogen was passed for 20 min. After the resultant mixture was copolymerized with methyl methacrylate and vinyl acetate for 1 h, added aluminum sulfate to break emulsion and then filtered, washed with water and alcohol, respectively, and vacuum dried to prepare the polymer [50]. The quasi-solid-state gel electrolyte was prepared as follows: 12% (wt%) of poly(methyl methacrylate-co-

vinyl acetate) and the liquid electrolyte were mixed in 3-methoxypropionitrile, heated at 60–70 °C for 1 h, then cooled and repeated several times, until all solids dissolved and a clear gel appeared.

4.3. Synthesis and characterization of the dyes

4.3.1. Synthesis of 11,12-bis(2-ethylhexyl)-11,12-dihydroindolo[2,3-a]carbazole (**2**)

To a stirred solution of 11,12-dihydroindolo[2,3-a]carbazole (2.00 g, 7.80 mmol) in 50 mL *N,N*-dimethylformamide (DMF) was added KOH (1.10 g, 19.64 mmol). The mixture was stirred for 30 min at room temperature under argon atmosphere. Then, 2-ethylhexyl bromide (3.37 mL, 19.64 mmol) was slowly injected. The resulting mixture was stirred continually for an additional 12 h. The reaction mixture was poured into water and extracted with CH₂Cl₂ (DCM). The organic phase was washed with brine and dried over anhydrous MgSO₄. After the solvent was removed, the product was purified by column chromatography on silica gel using petroleum ether (PE) as the eluent (yield: 87%, 3.29 g), mp 71–72 °C. ¹H NMR (CDCl₃, 600 MHz, ppm): δ 8.16 (d, *J* = 7.2 Hz, 2H), 7.96 (s, 2H), 7.56 (d, *J* = 7.8 Hz, 2H), 7.49–7.47 (m, 2H), 7.32–7.30 (m, 2H), 4.64–4.57 (m, 4H), 1.99–1.95 (m, 2H), 1.04–0.91 (m, 6H), 0.85–0.73 (m, 10H), 0.62–0.58 (m, 12H). ¹³C NMR (CDCl₃, 150 MHz, ppm): δ 142.87, 130.40, 126.06, 124.72, 124.04, 120.01, 119.86, 112.94, 111.92, 51.87, 38.15, 29.82, 27.80, 23.34, 22.80, 13.83, 10.20. HRMS (ESI, *m/z*): [M]⁺ calcd for [C₃₄H₄₄N₂]⁺: 480.3499, found: 480.3483.

4.3.2. Synthesis of 3-bromo-11,12-bis(2-ethylhexyl)-11,12-dihydroindolo[2,3-a]carbazole (**3**)

Under argon, compound **2** (1.66 g, 3.45 mmol) was dissolved in 100 mL DMF then *N*-bromosuccinimide (NBS) (615 mg, 3.45 mmol) was added at 0 °C. After 2 h of reaction, the temperature was gradually raised to room temperature, and the reaction was continued for 24 h. The reaction mixture was poured into water and extracted with DCM, and the organic phase washed with water, dried over anhydrous MgSO₄. After the solvent was removed, the product was purified by column chromatography on silica gel with PE as eluent to afford compound **3** as a yellow-green solid (yield: 97%, 1.88 g), mp 72–74 °C. ¹H NMR (CDCl₃, 600 MHz, ppm): δ 8.95 (d, *J* = 7.8 Hz, 1H), 8.09–8.08 (m, 2H), 7.57–7.47 (m, 4H), 7.37–7.34 (m, 1H), 7.32–7.29 (m, 1H), 4.60–4.54 (m, 4H), 1.90–1.83 (m, 2H), 0.97–0.88 (m, 6H), 0.77–0.65 (m, 10H), 0.59–0.54 (m, 12H). ¹³C NMR (CDCl₃, 150 MHz, ppm): δ 143.38, 142.76, 131.78, 129.61, 125.92, 125.42, 125.26, 124.83, 122.78, 121.32, 120.35, 120.24, 120.00, 116.99, 112.40, 111.97, 108.33, 52.09, 51.81, 38.00, 37.83, 29.81, 29.78, 27.74, 27.70, 27.07, 23.35, 22.77, 13.80, 10.15, 10.12. HRMS (ESI, *m/z*): [M]⁺ calcd for [C₃₄H₄₃BrN₂]⁺: 558.2604, found: 558.2605.

4.3.3. Synthesis of 11,12-bis(2-ethylhexyl)-3-(4,4,5,5-tetramethyl-1,3,2-dioxaborolan-2-yl)-11,12-dihydroindolo[2,3-a]carbazole (**4**)

Under argon, compound **3** (4.11 g 7.34 mmol), bis(pinacolato)diboron (B₂pin₂) (5.6 g, 22.05 mmol), anhydrous potassium acetate (KOAc) (2.16 g, 22.05 mmol), dichloro[1,1'-bis(diphenylphosphino)ferrocene]palladium(II) (Pd(dppf)Cl₂) (323 mg, 0.441 mmol) were dissolved in 1,4-dioxane (100 mL). The solution was stirred and heated at 80 °C for 24 h. After cooling, the solvent was distilled off under reduced pressure and the residue was poured into water and extracted with DCM, the organic extract was dried over MgSO₄. After the solvent was removed, the product was purified by column chromatography on silica gel using PE:DCM = 5:1 as the eluent to afford compound **4** as a brown viscous oil (yield: 97%, 1.88 g). ¹H NMR (CDCl₃, 600 MHz, ppm): δ 9.11 (d, *J* = 7.8 Hz, 1H), 8.47 (s, 1H), 8.19 (d, *J* = 7.8 Hz, 1H), 7.52–7.50 (m, 2H), 7.45–7.43 (m, 2H), 7.30–7.27 (m, 2H), 4.58–4.51 (m, 4H), 1.84–1.80 (m, 2H), 1.54 (s, 12H), 0.99–0.46 (m, 30H). ¹³C NMR (CDCl₃, 150 MHz, ppm): δ 143.14, 142.98, 142.97, 132.83, 130.82, 127.48, 126.33, 124.72, 124.53, 123.97, 123.14, 122.96, 120.43,

120.19, 119.73, 112.10, 111.90, 83.91, 51.93, 51.67, 37.97, 37.67, 29.95, 29.91, 27.98, 27.82, 25.28, 25.25, 25.22, 25.18, 23.31, 23.28, 22.82, 22.80, 13.89, 13.85, 10.04, 10.03.

4.3.4. Synthesis of 5-(5-(11,12-bis(2-ethylhexyl)-11,12-dihydroindolo[2,3-a]carbazol-3-yl)thieno[3,2-b]thiophen-2-yl)thiophene-2-carbaldehyde (**8**)

Under argon, compound **4** (756 mg, 1.25 mmol), compound **7** (300 mg, 0.91 mmol), tetrakis(triphenylphosphine)palladium(0) (63 mg, 0.055 mmol), potassium carbonate (502 mg, 3.64 mmol) were dissolved in a mixture of THF/water. The solution was stirred and heated to 80 °C for 16 h. After cooling, the reaction mixture was poured into water and extracted with DCM, and the organic phase washed with water, dried over anhydrous MgSO₄. The solvent was removed by rotary evaporation, **8** was obtained as an orange solid by column chromatography on silica gel using PE:DCM:Acetone = 40:20:1 as the eluent (yield: 56%, 440 mg), mp 78–81 °C. ¹H NMR (CDCl₃, 600 MHz, ppm): δ 9.90 (s, 1H), 8.11 (d, *J* = 7.2 Hz, 1H), 7.94 (s, 1H), 7.72 (d, *J* = 3.6 Hz, 1H), 7.67–7.65 (m, 2H), 7.57–7.54 (m, 2H), 7.50–7.47 (m, 1H), 7.46 (s, 1H), 7.43–7.41 (m, 1H), 7.34 (d, *J* = 4.2 Hz, 1H), 7.31–7.29 (m, 1H), 7.09–7.06 (m, 1H), 4.62–4.59 (m, 4H), 1.94–1.88 (m, 2H), 0.95–0.52 (m, 28H). ¹³C NMR (CDCl₃, 150 MHz, ppm): δ 182.53, 147.96, 147.74, 143.33, 143.02, 141.77, 140.08, 139.99, 137.52, 136.41, 130.80, 130.71, 125.90, 125.46, 125.27, 124.89, 124.20, 123.47, 122.28, 121.95, 121.74, 120.38, 120.22, 119.92, 119.24, 118.80, 116.23, 112.34, 112.20, 52.04, 51.92, 38.10, 38.01, 29.88, 29.80, 27.65, 27.59, 23.52, 23.49, 22.77, 22.76, 13.82, 13.80, 10.37, 10.31. HRMS (ESI, *m/z*): [M + K]⁺ calcd for [C₄₅H₄₈N₂OS₃K]⁺: 767.2560, found: 767.2563.

4.3.5. Synthesis of (E)-3-(5-(5-(11,12-bis(2-ethylhexyl)-11,12-dihydroindolo[2,3-a]carbazol-3-yl)thieno[3,2-b]thiophen-2-yl)thiophen-2-yl)-2-cyanoacrylic acid (**DC1**)

A mixture of compound **8** (420 mg, 0.576 mmol), *tert*-butyl cyanoacetate (244 mg, 1.73 mmol), ammonium acetate (133 mg, 1.73 mmol), and acetic acid (2 mL) in toluene (20 mL) was placed in a flask. The solution was stirred at reflux under argon atmosphere for 3.5 h. After cooling, the reaction was quenched by addition of water and the mixture was extracted with DCM. The organic layer was dried over anhydrous MgSO₄ and evaporated under vacuum. The ester intermediate was obtained as a red solid by column chromatography on silica gel using PE:DCM:Acetone = 40:20:1 as the eluent (yield: 71%, 348 mg). The ester intermediate was stirred with trifluoroacetic acid (20 mL) for 4 h, 100 mL of water was added and the resulting dark solid **DC1** was collected by filtration. The pure product was obtained by repeatedly water washing and centrifugation as a black powder (yield: 64%, 295 mg), mp 132–134 °C. ¹H NMR (THF-*d*₈, 600 MHz, ppm): δ 10.82 (s, 1H), 8.37 (s, 1H), 8.13 (d, *J* = 7.8 Hz, 1H), 7.99 (s, 1H), 7.92 (s, 1H), 7.86 (d, *J* = 3.6 Hz, 1H), 7.66–7.61 (m, 3H), 7.53–7.52 (m, 1H), 7.48 (d, *J* = 3.6 Hz, 1H), 7.45–7.42 (m, 1H), 7.37–7.34 (m, 1H), 7.26–7.23 (m, 1H), 7.02–6.99 (m, 1H), 4.71–4.68 (m, 4H), 1.96–1.91 (m, 2H), 0.96–0.48 (m, 28H). ¹³C NMR (THF-*d*₈, 150 MHz, ppm): δ 164.17, 148.67, 148.11, 146.47, 144.51, 144.24, 141.37, 141.17, 140.24, 137.37, 135.92, 131.87, 131.75, 126.98, 126.46, 126.15, 125.75, 125.34, 124.61, 123.14, 122.97, 122.91, 121.28, 121.02, 120.78, 120.42, 120.19, 117.07, 116.81, 113.38, 113.21, 99.99, 52.69, 52.59, 39.14, 39.05, 30.71, 30.46, 28.66, 28.23, 24.41, 24.27, 23.69, 23.64, 14.21, 14.15, 10.75, 10.48. HRMS (ESI, *m/z*): [M + NH₄]⁺ calcd for [C₄₈H₅₃N₄O₂S₃]⁺: 813.3325, found: 813.3305.

4.3.6. Synthesis of 5''-(11,12-bis(2-ethylhexyl)-11,12-dihydroindolo[2,3-a]carbazol-3-yl)-[2,2':5',2''-terthiophene]-5-carbaldehyde (**10**)

Under argon, compound **4** (700 mg, 1.15 mmol), compound **9** (300 mg, 0.84 mmol), tetrakis(triphenylphosphine)palladium(0) (57 mg, 0.049 mmol), potassium carbonate (466 mg, 3.38 mmol) were dissolved in a mixture of THF/water. The solution was stirred and

heated to 80 °C for 16 h. After cooling, the reaction mixture was poured into water and extracted with DCM, and the organic phase washed with water, dried over anhydrous MgSO₄. The solvent was removed by rotary evaporation, **10** was obtained as a dark red solid by column chromatography on silica gel using PE:DCM = 2:1 as the eluent (yield: 95%, 608 mg), mp 80–81 °C. ¹H NMR (CDCl₃, 600 MHz, ppm): δ 9.87 (s, 1H), 8.11 (d, *J* = 7.2 Hz, 1H), 7.92 (s, 1H), 7.77 (d, *J* = 8.4 Hz, 1H), 7.68 (d, *J* = 4.2 Hz, 1H), 7.57–7.54 (m, 2H), 7.50–7.47 (m, 1H), 7.44–7.41 (m, 1H), 7.37 (d, *J* = 3.6 Hz, 1H), 7.32–7.25 (m, 4H), 7.22–7.21 (m, 1H), 7.13–7.10 (m, 1H), 4.62–4.58 (m, 4H), 1.94–1.88 (m, 2H), 0.95–0.71 (m, 16H), 0.64–0.52 (m, 12H). ¹³C NMR (CDCl₃, 150 MHz, ppm): δ 182.52, 147.17, 143.86, 143.34, 142.98, 141.61, 139.87, 137.54, 136.10, 134.22, 130.87, 130.56, 128.00, 127.17, 125.93, 125.59, 125.20, 124.81, 124.72, 124.45, 124.09, 123.53, 122.29, 121.93, 121.39, 120.32, 120.19, 119.84, 116.05, 112.32, 112.15, 52.00, 51.86, 38.07, 37.98, 29.84, 29.80, 23.50, 23.47, 22.83, 22.77, 22.75, 22.73, 13.81, 13.79, 10.29, 10.16. HRMS (ESI, *m/z*): [M]⁺ calcd for [C₄₇H₅₀N₂O₃S]⁺: 754.3080, found: 754.3055.

4.3.7. Synthesis of (E)-3-(5''-(11,12-bis(2-ethylhexyl)-11,12-dihydroindolo[2,3-a]carbazol-3-yl)-[2,2':5',2''-terthiophen]-5-yl)-2-cyanoacrylic acid (DC2)

A mixture of compound **10** (560 mg, 0.74 mmol), *tert*-butyl cyanoacetate (314 mg, 2.22 mmol), ammonium acetate (172 mg, 2.22 mmol), and acetic acid (2 mL) in toluene (20 mL) was placed in a flask. The solution was stirred at reflux under argon atmosphere for 3.5 h. After cooling, the reaction was quenched by addition of water and the mixture was extracted with DCM. The organic layer was dried over anhydrous MgSO₄ and evaporated under vacuum. The ester intermediate was obtained as a red solid by column chromatography on silica gel using PE:DCM:Acetone = 40:20:1 as the eluent (yield: 77%, 503 mg). The ester intermediate was stirred with trifluoroacetic acid (20 mL) for 4 h, 100 mL of water was added and the resulting red solid **DC2** was collected by filtration. The pure product was obtained by repeatedly water washing and centrifugation as a dark red powder (yield: 71%, 435 mg), mp 125–127 °C. ¹H NMR (THF-*d*₈, 600 MHz, ppm): δ 10.83 (s, 1H), 8.35 (s, 1H), 8.12 (d, *J* = 7.8 Hz, 1H), 7.94 (s, 1H), 7.82 (d, *J* = 4.2 Hz, 1H), 7.74 (d, *J* = 7.8 Hz, 1H), 7.64–7.61 (m, 2H), 7.50–7.47 (m, 2H), 7.45–7.42 (m, 2H), 7.39–7.33 (m, 2H), 7.25–7.23 (m, 2H), 7.05–7.03 (m, 1H), 4.73–4.67 (m, 4H), 1.95–1.91 (m, 2H), 0.95–0.47 (m, 28H). ¹³C NMR (THF-*d*₈, 150 MHz, ppm): δ 164.14, 147.17, 146.49, 144.79, 144.50, 144.21, 140.59, 140.38, 137.19, 135.83, 135.22, 131.93, 131.63, 129.06, 128.46, 126.99, 126.57, 126.10, 125.89, 125.72, 125.69, 125.37, 124.66, 123.11, 122.94, 122.39, 121.24, 120.99, 120.71, 116.92, 116.78, 113.37, 113.20, 99.90, 52.63, 52.60, 39.12, 39.03, 30.70, 30.53, 28.40, 28.21, 24.34, 24.27, 23.68, 23.65, 14.21, 14.19, 10.75, 10.63. HRMS (ESI, *m/z*): [M + NH₄]⁺ calcd for [C₅₀H₅₅N₄O₂S₃]⁺: 839.3482, found: 839.3518.

4.3.8. Synthesis of 5''-(11,12-bis(2-ethylhexyl)-11,12-dihydroindolo[2,3-a]carbazol-3-yl)-3,3''-dihexyl-[2,2':5',2''-terthiophene]-5-carbaldehyde (15)

Under argon, compound **4** (486 mg, 0.8 mmol), compound **14** (300 mg, 0.57 mmol), tetrakis(triphenylphosphine)palladium(0) (40 mg, 0.035 mmol), potassium carbonate (317 mg, 2.3 mmol) were dissolved in a mixture of THF/water. The solution was stirred and heated to 80 °C for 16 h. After cooling, the reaction mixture was poured into water and extracted with DCM, and the organic phase washed with water, dried over anhydrous MgSO₄. The solvent was removed by rotary evaporation, **15** was obtained as an orange solid by column chromatography on silica gel using PE:Acetone = 20:1 as the eluent (yield: 36%, 194 mg), mp 90–93 °C. ¹H NMR (CDCl₃, 600 MHz, ppm): δ 9.85 (s, 1H), 8.10 (d, *J* = 7.8 Hz, 1H), 7.92 (s, 1H), 7.85 (d, *J* = 7.8 Hz, 1H), 7.62 (s, 1H), 7.56–7.54 (m, 2H), 7.49–7.46 (m, 1H), 7.45–7.42 (m, 1H), 7.31–7.28 (m, 2H), 7.24 (d, *J* = 3.6 Hz, 1H), 7.20 (s, 1H), 7.14–7.11 (m, 1H), 4.61–4.57 (m, 4H), 2.95–2.92 (m, 2H), 2.88 (t,

J = 7.8 Hz, 2H), 1.92–1.89 (m, 2H), 1.83–1.71 (m, 4H), 1.51–1.44 (m, 4H), 1.37–1.34 (m, 8H), 0.92–0.73 (m, 22H), 0.63–0.53 (m, 12H). ¹³C NMR (CDCl₃, 150 MHz, ppm): δ 182.66, 143.34, 142.98, 142.27, 141.54, 140.54, 140.34, 140.22, 139.25, 139.12, 134.17, 130.90, 130.44, 130.36, 129.63, 128.04, 126.05, 125.98, 125.69, 125.13, 124.73, 123.57, 122.36, 121.81, 121.71, 120.26, 120.20, 119.72, 115.91, 112.30, 112.14, 52.01, 51.82, 38.05, 37.94, 31.93, 31.80, 30.89, 30.48, 29.92, 29.85, 29.66, 29.49, 29.35, 27.78, 27.52, 23.53, 23.47, 23.44, 22.82, 22.78, 22.76, 14.27, 14.23, 13.84, 13.82, 10.34, 10.27, 10.16. HRMS (ESI, *m/z*): [M + Na]⁺ calcd for [C₅₉H₇₄N₂O₃Na]⁺: 945.4856, found: 945.4827.

4.3.9. Synthesis of (E)-3-(5''-(11,12-bis(2-ethylhexyl)-11,12-dihydroindolo[2,3-a]carbazol-3-yl)-3,3''-dihexyl-[2,2':5',2''-terthiophen]-5-yl)-2-cyanoacrylic acid (DC3)

A mixture of compound **15** (166 mg, 0.18 mmol), *tert*-butyl cyanoacetate (76 mg, 0.54 mmol), ammonium acetate (42 mg, 0.54 mmol), and acetic acid (2 mL) in toluene (20 mL) was placed in a flask. The solution was stirred at reflux under argon atmosphere for 3.5 h. After cooling, the reaction was quenched by addition of water and the mixture was extracted with DCM. The organic layer was dried over anhydrous MgSO₄ and evaporated under vacuum. The ester intermediate was obtained as a red solid by column chromatography on silica gel using PE:DCM:Acetone = 60:30:1 as the eluent (yield: 66%, 125 mg). The ester intermediate was stirred with trifluoroacetic acid (20 mL) for 4 h, 100 mL of water was added and the resulting dark solid **DC3** was collected by filtration. The pure product was obtained by repeatedly water washing and centrifugation as a brown powder (yield: 51%, 92 mg), mp 145–147 °C. ¹H NMR (THF-*d*₈, 600 MHz, ppm): δ 8.31 (s, 1H), 8.13 (d, *J* = 7.8 Hz, 1H), 7.94 (s, 1H), 7.82 (d, *J* = 7.8 Hz, 1H), 7.78 (s, 1H), 7.64–7.62 (m, 2H), 7.45–7.42 (m, 2H), 7.39–7.36 (m, 1H), 7.31 (d, *J* = 3.6 Hz, 1H), 7.26–7.22 (m, 2H), 7.07–7.04 (m, 1H), 4.71–4.67 (m, 4H), 2.99–2.91 (m, 4H), 1.95–1.93 (m, 2H), 1.85–1.80 (m, 2H), 1.78–1.74 (m, 2H), 1.55–1.45 (m, 4H), 1.39–1.29 (m, 10H), 0.92–0.48 (m, 32H). ¹³C NMR (THF-*d*₈, 150 MHz, ppm): δ 164.15, 146.40, 144.50, 144.17, 143.43, 142.04, 141.56, 141.46, 141.29, 139.93, 135.03, 134.60, 131.94, 131.53, 131.37, 130.61, 129.35, 127.28, 127.03, 126.64, 126.06, 125.64, 124.68, 123.17, 122.80, 122.64, 121.22, 120.98, 120.62, 116.77, 116.68, 113.37, 113.19, 100.07, 52.62, 52.48, 39.08, 38.96, 32.94, 32.82, 31.86, 31.32, 30.68, 30.44, 30.32, 30.25, 28.38, 28.22, 24.27, 24.21, 23.76, 23.71, 23.68, 23.67, 14.67, 14.63, 14.25, 14.22, 14.18, 10.72, 10.60, 10.46. HRMS (ESI, *m/z*): [M]⁺ calcd for [C₆₂H₇₅N₃O₂S₃]⁺: 989.5016, found: 989.5052.

Acknowledgments

This work was financially supported by the NSFC (21462054 and 61368006); Supported by the Scientific Research Fund of Guizhou Provincial Science and Technology Department (LH[2015]7036 and [2015]4003); Supported by the Science and Technology Cooperation talent Project of Zunyi City, China ([2016]14).

Appendix A. Supplementary data

Supplementary data to this article can be found online at <https://doi.org/10.1016/j.dyepig.2019.01.033>.

References

- [1] Gao F, Wang Y, Shi D, Zhang J, Wang M, Jing X, et al. Enhance the optical absorptivity of nanocrystalline TiO₂ film with high molar extinction coefficient ruthenium sensitizers for high performance dye-sensitized solar cells. *J Am Chem Soc* 2008;130:10720–8 <https://doi.org/10.1021/ja801942j>.
- [2] Nazeeruddin MK, Péchy P, Renouard T, Zakeeruddin SM, Humphry-Baker R, Comte P, et al. Engineering of efficient panchromatic sensitizers for nanocrystalline TiO₂-based solar cells. *J Am Chem Soc* 2001;123:1613–24 <https://doi.org/10.1021/>

- ja003299u.
- [3] Wang P, Klein C, Humphry-Baker R, Zakeeruddin SM, Grätzel M. A high molar extinction coefficient sensitizer for stable dye-sensitized solar cells. *J Am Chem Soc* 2005;127:808–9 <https://doi.org/10.1021/ja0436190>.
 - [4] Wang Y, Chen B, Wu W, Li X, Zhu W, Tian H, et al. Efficient solar cells sensitized by porphyrins with an extended conjugation framework and a carbazole donor: from molecular design to cosensitization. *Angew Chem Int Ed* 2014;53:1–6 <https://doi.org/10.1002/anie.201406190>.
 - [5] Xie Y, Tang Y, Wu W, Wang Y, Liu Jingchuan, Li X, et al. Porphyrin cosensitization for a photovoltaic efficiency of 11.5%: a record for non-ruthenium solar cells based on iodine electrolyte. *J Am Chem Soc* 2015;137:14055–8 <https://doi.org/10.1021/jacs.5b09665>.
 - [6] Mathew S, Yella A, Gao P, Humphry-Baker R, Curchod Basile FE, Ashari-Astani N, et al. Dye-sensitized solar cells with 13% efficiency achieved through the molecular engineering of porphyrin sensitizers. *Nat Chem* 2014;6:242–7 <https://doi.org/10.1038/NCHEM.1861>.
 - [7] Yella A, Lee H-W, Tsao HN, Yi C, Chandiran AK, Nazeeruddin MK, et al. Porphyrin-sensitized solar cells with cobalt (II/III)-Based redox electrolyte exceed 12 percent efficiency. *Science* 2011;334:629–34 <https://doi.org/10.1126/science.1209688>.
 - [8] Qin H, Wenger S, Xu M, Gao F, Jing X, Wang P, et al. An organic sensitizer with a fused dithienothiophene unit for efficient and stable dye-sensitized solar cells. *J Am Chem Soc* 2008;130:9202–3 <https://doi.org/10.1021/ja8024438>.
 - [9] Thomas KRJ, Hsu Y-C, Lin JT, Lee K-M, Ho K-C, Lai C-H, et al. 2,3-Disubstituted thiophene-based organic dyes for solar cells. *Chem Mater* 2008;20:1830–40 <https://doi.org/10.1021/cm702631r>.
 - [10] Tang J, Wu W, Hua J, Li J, Li X, Tian H. Starburst triphenylamine-based cyanine dye for efficient quasi-solid-state dye-sensitized solar cells. *Energy Environ Sci* 2009;2:982–90 <https://doi.org/10.1039/b906596b>.
 - [11] Yang H-Y, Yen Y-S, Hsu Y-C, Chou H-H, Lin JT. Organic dyes incorporating the dithieno[3,2-b:2',3'-d]thiophene moiety for efficient dye-sensitized solar cells. *Org Lett* 2010;12:16–9 <https://doi.org/10.1021/ol902327p>.
 - [12] Bolag A, Nishida J-i, Hara K, Yamashita Y. Dye-sensitized solar cells based on novel diphenylpyran derivatives. *Chem Lett* 2011;40(5):510–1 <https://doi.org/10.1246/cl.2011.510>.
 - [13] Li W, Wu Y, Li X, Xie Y, Zhu W. Absorption and photovoltaic properties of organic solar cell sensitizers containing fluorene unit as conjugation bridge. *Energy Environ Sci* 2011;4:1830–7 <https://doi.org/10.1039/c0ee00788a>.
 - [14] Franco S, Garin J, NMnd Baroja, Pérez-Tejada R, Orduna J, Yu Y, et al. New D- π -A-Conjugated organic sensitizers based on 4H-Pyran-4-ylidene donors for highly efficient dye-sensitized solar cells. *Org Lett* 2012;14:752–5 <https://doi.org/10.1021/ol203298r>.
 - [15] Mao J, He N, Ning Z, Zhang Q, Guo F, Chen L, et al. Stable dyes containing double acceptors without COOH as anchors for highly efficient dye-sensitized solar cells. *Angew Chem Int Ed* 2012;51:9873–6 <https://doi.org/10.1002/anie.201204948>.
 - [16] Cai N, Zhang J, Xu M, Zhang M, Wang P. Improving the photovoltage of dithienopyrrole dye-sensitized solar cells via attaching the bulky bis(octyloxy)biphenyl moiety to the conjugated π -linker. *Adv Funct Mater* 2013;23:3539–47 <https://doi.org/10.1002/adfm.201203348>.
 - [17] Lee M-W, Kim J-Y, Lee D-H, Ko MJ. Novel D- π -A organic dyes with thieno[3,2-b]thiophene-3,4-ethylenedioxythiophene unit as a π -bridge for highly efficient dye-sensitized solar cells with long-term stability. *ACS Appl Mater Interfaces* 2014;6:4102–8 <https://doi.org/10.1021/am405686z>.
 - [18] Yao Z, Zhang M, Wu H, Yang L, Li R, Wang P. Donor/Acceptor indenoperylene dye for highly efficient organic dye-sensitized solar cells. *J Am Chem Soc* 2015;137:3799–802 <https://doi.org/10.1021/jacs.5b01537>.
 - [19] Demeter D, Roncali J, Jungsttviwong S, Melchiorre F, Biagini P, Po R. Linearly π -conjugated oligothiophenes as simple metal-free sensitizers for dye-sensitized solar cells. *J Mater Chem C* 2015;3(29):7756–61 <https://doi.org/10.1039/c5tc01183c>.
 - [20] Demeter D, Melchiorre F, Biagini P, Jungsttviwong S, Po R, Roncali J. 3,4-Ethylenedioxythiophene (EDOT) and 3,4-ethylenedithiathiophene (EDIT) as terminal blocks for oligothiophene dyes for DSSCs. *Tetrahedron Lett* 2016;57(43):4815–20 <https://doi.org/10.1016/j.tetlet.2016.09.053>.
 - [21] Zhang H, Iqbal Z, Chen Z-E, Hong Y. Effects of various heteroatom donor species on the photophysical, electrochemical and photovoltaic performance of dye-sensitized solar cells. *Electrochim Acta* 2018;290:303–11 <https://doi.org/10.1016/j.electacta.2018.08.068>.
 - [22] Dessì A, Calamante M, Mordini A, Peruzzini M, Sinicropi A, Basosi R, et al. Organic dyes with intense light absorption especially suitable for application in thin-layer dye-sensitized solar cells. *Chem Commun* 2014;50:13952–5 <https://doi.org/10.1039/c4cc06160h>.
 - [23] Grisorio R, Marco LD, Agosta R, Iacobellis R, Giannuzzi R, Manca M, et al. Enhancing dye-sensitized solar cell performances by molecular engineering: highly efficient π -extended organic sensitizers. *ChemSusChem* 2014;7:2659–69 <https://doi.org/10.1002/cssc.201402164>.
 - [24] Huang J-H, Jiang K-J, Zhang F, Wu W, Li S-G, Yang L-M, et al. Engineering diketopyrrolopyrrole sensitizers for highly efficient dye-sensitized solar cells: enhanced light harvesting and intramolecular charge transfer. *RSC Adv* 2014;4:16906–12 <https://doi.org/10.1039/c4ra02009j>.
 - [25] Mahmood A. Triphenylamine based dyes for dye sensitized solar cells: a review. *Sol Energy* 2016;123:127–44 <https://doi.org/10.1016/j.solener.2015.11.015>.
 - [26] Godfroy M, Aumaitre C, Caffy F, Kervella Y, Cabau L, Pellejà L, et al. Dithienylpyrazine-based photosensitizers: effect of swapping a connecting unit on optoelectronic properties and photovoltaic performances. *Dyes Pigments* 2017;146:352–60 <https://doi.org/10.1016/j.dyepig.2017.07.022>.
 - [27] Jia J, Chen Y, Duan L, Sun Z, Liang M, Xue S. New D- π -A dyes incorporating dithieno[3,2-b:2',3'-d]pyrrole (DTP)-based π -spacers for efficient dye-sensitized solar cells. *RSC Adv* 2017;7:45807–17 <https://doi.org/10.1039/c7ra08965a>.
 - [28] Fang J-K, Hu X, Xu M, Wang H, Zhang Y, Jin C, et al. Molecular engineering of efficient organic sensitizers containing diyne-bridge for dye-sensitized solar cells. *Electrochim Acta* 2017;253:572–80 <https://doi.org/10.1016/j.electacta.2017.09.098>.
 - [29] Ma L-W, Huang Z-S, Wang S, Meier H, Cao D. Impact of π -conjugation configurations on the photovoltaic performance of the quinoxaline-based organic dyes. *Dyes Pigments* 2017;145:126–35 <https://doi.org/10.1016/j.dyepig.2017.05.054>.
 - [30] Lee H, Kim J, Kim DY, Seo Y. Co-sensitization of metal free organic dyes in flexible dye-sensitized solar cells. *Org Electron* 2018;52:103–9 <https://doi.org/10.1016/j.orgel.2017.10.003>.
 - [31] Wang X, Guo L, Xia PF, Zheng F, Wong MS, Zhu Z. Effects of surface modification on dye-sensitized solar cell based on an organic dye with naphtho[2,1-b:3,4-b']dithiophene as the conjugated linker. *ACS Appl Mater Interfaces* 2014;6:1926–32 <https://doi.org/10.1021/am404984g>.
 - [32] Sousa SD, Lyu S, Ducasse L, Toupance T, Olivier C. Tuning visible-light absorption properties of Ru-diacetylidyde complexes: simple access to colorful efficient dyes for DSSCs. *J Mater Chem* 2015;3:18256–64 <https://doi.org/10.1039/c5ta04498g>.
 - [33] Luo G-G, Lu H, Wang Y-H, Dong J, Zhao Y, Wu R-B. A D- π -A- π -A metal-free organic dye with improved efficiency for the application of solar energy conversion. *Dyes Pigments* 2016;134:498–505 <https://doi.org/10.1016/j.dyepig.2016.08.013>.
 - [34] Bonomo M, Carlo AD, Centore R, Dini D, Carella A. New pyran-based dyes as efficient sensitizers of p-type dye-sensitized solar cells. *Sol Energy* 2018;169:237–41 <https://doi.org/10.1016/j.solener.2018.04.050>.
 - [35] Capodilupo AL, Fabiano E, Marco LD, Ciccarella G, Gigli G, Martinelli C, et al. [1] Benzothieno[3,2-b]benzothiophene-Based organic dyes for dye-sensitized solar cells. *J Org Chem* 2016;81:3235–45 <https://doi.org/10.1021/acs.joc.6b00192>.
 - [36] Imae I, Koshima T, Korai K, Ooyama Y, Komaguchi K, Harima Y. Enhanced photovoltaic performances of panchromatic EDOT-containing dye by introducing bulky dialkylfluorene units in donor moiety. *Dyes Pigments* 2016;132:262–9 <https://doi.org/10.1016/j.dyepig.2016.05.014>.
 - [37] Iqbal Z, Wu W-Q, Huang Z-S, Wang L, Kuang D-B, Meier H, et al. Trilateral π -conjugation extensions of phenothiazine-based dyes enhance the photovoltaic performance of the dye-sensitized solar cells. *Dyes Pigments* 2016;124:63–71 <https://doi.org/10.1016/j.dyepig.2015.09.001>.
 - [38] Maglione C, Carella A, Carbonara C, Centore R, Fusco S, Velardo A, et al. Novel pyran based dyes for application in dye sensitized solar cells. *Dyes Pigments* 2016;133:395–405 <https://doi.org/10.1016/j.dyepig.2016.06.024>.
 - [39] Huang Z-S, Meier H, Cao D. Phenothiazine-based dyes for efficient dye-sensitized solar cells. *J Mater Chem C* 2016;4(13):2404–26 <https://doi.org/10.1039/c5tc04418a>.
 - [40] Zhang C, Wang S, Li Y. Phenothiazine organic dyes containing dithieno[3,2-b:2',3'-d]pyrrole (DTP) units for dye-sensitized solar cells. *Sol Energy* 2017;157:94–102 <https://doi.org/10.1016/j.solener.2017.08.012>.
 - [41] Meier H, Huang Z-S, Cao D. Double D- π -A branched dyes – a new class of metal-free organic dyes for efficient dye-sensitized solar cells. *J Mater Chem C* 2017;5(38):9828–37 <https://doi.org/10.1039/c7tc03406g>.
 - [42] Yang S, Guan D, Yang M, Tian J, Chu W, Sun Z. Synthesis and characterization of novel butterfly-shaped aryl-substituted indolo[2,3-a]carbazole derivatives. *Tetrahedron Lett* 2015;56:2223–7 <https://doi.org/10.1016/j.tetlet.2015.03.058>.
 - [43] Zhu S, An Z, Chen X, Chen P, Liu Q. Cyclic thiourea functionalized dyes with binary π -linkers: influence of different π -conjugation segments on the performance of dye-sensitized solar cells. *Dyes Pigments* 2015;116:146–54 <https://doi.org/10.1016/j.dyepig.2015.01.022>.
 - [44] Wei Y, Yang Y, Yeh J-M. Synthesis and electronic properties of aldehyde end-capped thiophene oligomers and other ω -substituted seshithiophenes. *Chem Mater* 1996;8:2659–66 <https://doi.org/10.1021/cm960182p>.
 - [45] Kim K-H, Yu H, Kang H, Kang DJ, Cho C-H, Cho H-H, et al. Influence of intermolecular interactions of electron donating small molecules on their molecular packing and performance in organic electronic devices. *J Mater Chem* 2013;1:14538–47 <https://doi.org/10.1039/c3ta13266h>.
 - [46] Qian X, Zhu Y-Z, Song J, Gao X-P, Zheng J-Y. New Donor- π -Acceptor type triazatruxene derivatives for highly efficient dye-sensitized solar cells. *Org Lett* 2013;15:6034–7 <https://doi.org/10.1021/ol402931u>.
 - [47] Cai S, Tian G, Li X, Su J, Tian H. Efficient and stable DSSC sensitizers based on substituted dihydroindolo[2,3-b]carbazole donors with high molar extinction coefficients. *J Mater Chem* 2013;1(37):11295–305 <https://doi.org/10.1039/c3ta11748k>.
 - [48] Qian X, Shao L, Li H, Yan R, Wang X, Hou L. Indolo[3,2-b]carbazole-based multi-donor- π -acceptor type organic dyes for highly efficient dye-sensitized solar cells. *J Power Sources* 2016;319:39–47 <https://doi.org/10.1016/j.jpowsour.2016.04.043>.
 - [49] Zhang H, Fan J, Iqbal Z, Kuang D-B, Wang L, Meier H, et al. Novel dithieno[3,2-b:2',3'-d]pyrrole-based organic dyes with high molar extinction coefficient for dye-sensitized solar cells. *Org Electron* 2013;14(8):2071–81 <https://doi.org/10.1016/j.orgel.2013.04.046>.
 - [50] Wang C, Wang L, Shi Y, Zhang H, Ma T. Printable electrolytes for highly efficient quasi-solid-state dye-sensitized solar cells. *Electrochim Acta* 2013;91:302–6 <https://doi.org/10.1016/j.electacta.2012.12.096>.